Synthesis of Trifluoromethylaryl Diazirine and Benzophenone Derivatives of Etomidate that Are Potent General Anesthetics and Effective Photolabels for Probing Sites on Ligand-Gated Ion Channels

S. Shaukat Husain,[†] Selvanayagam Nirthanan,[§] Dirk Ruesch,[†] Ken Solt,[†] Qi Cheng,[†] Guo-Dong Li,[#] Enrique Arevalo,[†] Richard W. Olsen,[#] Douglas E. Raines,[†] Stuart A. Forman,[†] Jonathan B. Cohen,[§] and Keith W. Miller,*[,‡]

Department of Anesthesia and Critical Care, Massachusetts General Hospital, Boston, Massachusetts 02114, Department of Biological Chemistry and Molecular Pharmacology, Department of Neurobiology, Harvard Medical School, Boston, Massachusetts 02115, and Department of Molecular and Medical Pharmacology, UCLA School of Medicine, Los Angeles, California 90095

Received November 30, 2005

To locate the binding sites of general anesthetics on ligand-gated ion channels, two derivatives of the intravenous general anesthetic etomidate (2-ethyl 1-(phenylethyl)-1*H*-imidazole-5-carboxylate), in which the 2-ethyl group has been replaced by photoactivable groups based on either aryl diazirine or benzophenone chemistry, have been synthesized and characterized pharmacologically. TDBzl−etomidate (4-[3-(trifluoromethyl)-3*H*-diazirin-3-yl]benzyl 1-(1-phenylethyl)-1*H*-imidazole-5-carboxylate) and BzBzl−etomidate (4-benzoylbenzyl-1-(1-phenylethyl)-1*H*-imidazole-5-carboxylate are both potent general anesthetics with half-effective anesthetic concentrations of 700 and 220 nM, respectively. Both agents resembled etomidate in enhancing currents elicited by low concentrations of GABA on heterologously expressed $GABA_A$ receptors and in shifting the GABA concentration−response curve to lower concentrations. They also allosterically enhanced the binding of flunitrazepam to mammalian brain $GABA_A$ receptors. Both agents were also effective and selective photolabels, photoincorporating into some, but not all, subunits of the *Torpedo* nicotinic acetylcholine receptor to a degree that was allosterically regulated by an agonist or a noncompetitive inhibitor. Thus, they have the necessary pharmacological and photochemical properties to be useful in identifying the site of etomidate-induced anesthesia.

Introduction

The intravenous agent, etomidate[a] (2-ethyl 1-(phenylethyl)-1*H*-imidazole-5-carboxylate), is one of the most potent general anesthetic agents in clinical use today causing anesthesia with a half-effective concentration of ∼2 μM.[1,2] Unlike the inhaled anesthetics, which act on a number of different ion channels at clinical concentrations, its mode of action is much more selective.[3] On the Cys-loop ion channel superfamily of receptors, which include subtypes activated by GABA, glycine, serotonin, and acetylcholine, it appears to act at the lowest concentrations on $GABA_A$ receptors but also affects the other members at somewhat higher concentrations.[4] At the $GABA_A$ receptor, it enhances GABA-induced currents by increasing the receptor's open probability, resulting in a shift in the agonist concentration−response curve to lower concentrations.[5] Enhancement is β-subunit-dependent and greater for the β_2- and β_3-subunits than for the β_1-subunit. Chimeras of these subunits demonstrated that enhancement could be attenuated by a single mutation in the second transmembrane helix of the β_2- or β_3-subunit.[6,7] Knock-in mice containing this mutation in the β_2-subunit are less sensitive to the sedative−hypnotic effects of etomidate[8] and in the β_3-subunit are less sensitive to many anesthetic effects of etomidate.[9] However, it is unclear whether this mutation is located in etomidate's binding site or whether it acts indirectly and allosterically on gating to reduce the effect of etomidate.[10]

An approach to locating the actual binding site is to develop photoactivable derivatives of etomidate and to use these to identify photoincorporation sites in relevant ion channels. One such agent, azietomidate [2-(3-methyl-3*H*-diaziren-3-yl)ethyl 1-(1-phenylethyl)-1*H*-imidazole-5-carboxylate], in which an ethoxy group has been replaced by a 3-azibutoxy group, has been synthesized previously.[11] It exhibits very similar potency and pharmacology to the parent compound both in tadpoles and rodents. Furthermore, in knock-in mice bearing the above-mentioned mutation in the β_3-subunit of the $GABA_A$ receptor, its potency compared to wild type is attenuated in parallel with that of etomidate.[12] Azietomidate has been successfully used to photolabel the abundant *Torpedo* nicotinic acetylcholine receptor (nAcChoR).[11] The latter receptors are photolabeled in an agonist-dependent manner, and photoincorporation is subunit-dependent. Residues in two different regions of the nAcChoR have photoincorporated azietomidate.[13] In the transmembrane region, there is binding in the ion channel, and in the extracellular region, there is low affinity binding in the agonist-binding pocket. The success of this agent is very encouraging, but the results obtained for this ligand, as well as with azialkanols, suggested that the reactive intermediates produced upon photolysis of the aliphatic diazirines react most efficiently with the nucleophilic amino acid side chains, Glu, Asp, His, and Tyr.[13−16] Although the alkyl diazirine is the least sterically perturbing photoactivable group available, successful application of this method to less abundant neuronal receptors would be greatly facilitated by the development of derivatives of general anesthetics that photoincorporate both with higher efficiency and into a broader range of amino acid side chains.

In this study we have synthesized and characterized two new etomidate derivatives in which the alkyl diazirine has been

* Corresponding author. Phone: (617) 726-8985. Fax: (617) 726-8644. E-mail: k_miller@helix.mgh.harvard.edu.
[†] Massachusetts General Hospital.
[‡] Department of Biological Chemistry and Molecular Pharmacology, Harvard Medical School.
[§] Department of Neurobiology, Harvard Medical School.
[#] UCLA School of Medicine.

10.1021/jm051207b CCC: $33.50
Published on Web 07/07/2006

Scheme 1. Synthesis of TDBzl−Etomidate

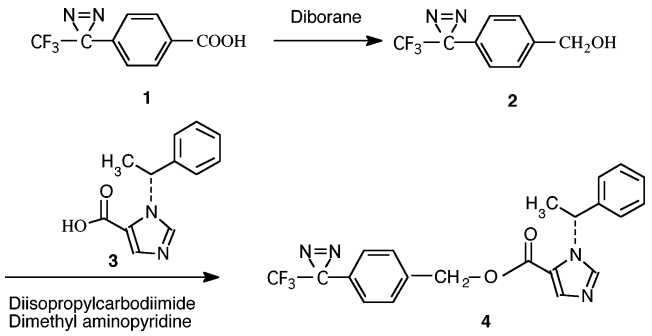

Scheme 2. Synthesis of BzBzl−Etomidate

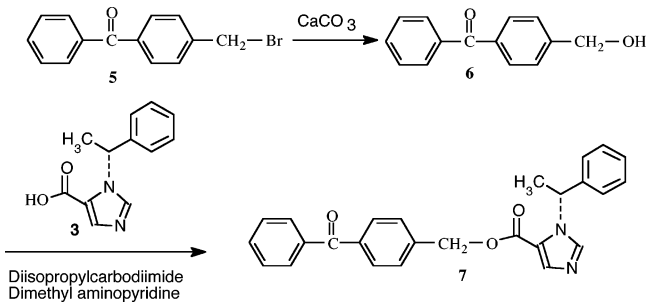

replaced by either a benzophenone or an aryl diazirine moiety, either of which upon photoactivation can also incorporate with high efficiency into normally unreactive aliphatic side chains.[17−19] Here, we show that, despite the larger substituent groups, these agents are potent general anesthetics that exert pharmacological actions on members of the Cys-loop ion channel superfamily of receptors. Furthermore, they both photoincorporate in an agonist- and subunit-dependent manner into nicotinic acetylcholine receptors.

Chemistry

Our aim was to synthesize and evaluate photoactivable analogues of the general anesthetic etomidate that would photoincorporate into a different spectrum of amino acid residues than the aliphatic diazirinyl derivative we previously used for photolabeling general anesthetic sites on acetylcholine and $GABA_A$ receptors.[13,14,20] For this purpose, we chose to incorporate trifluoromethylaryl diazirine and benzophenone photoreactive groups into the etomidate backbone to give two new photoreactive general anesthetics, *R*-4-[3-(trifluoromethyl)-3*H*-diazirin-3-yl]benzyl-1-(1-phenylethyl)-1*H*-imidazole-5-carboxylate **4** (TDBzl−etomidate, Scheme 1) and *R*-4-benzoylbenzyl-1-(1-phenylethyl)-1*H*-imidazole-5-carboxylate **7** (BzBzl−etomidate, Scheme 2), respectively. The strategy for the synthesis of these derivatives was to couple *R*-1-(1-phenylethyl)-1*H*-imidazole-5-carboxylic acid (**3**), obtained by alkaline cleavage of the ester bond of *R*-2-ethyl-1-(1-phenylethyl)-1*H*-imidazole-5-carboxylate (etomidate), with the appropriate hydroxyl group-containing component, 4-[3-(trifluoromethyl)-3*H*-diazirin-3-yl]benzyl alcohol, **2** (Scheme 1) or 4(hydroxymethyl)benzophenone, **6** (Scheme 2). 4-[3-(Trifluoromethyl)-3*H*-diazirin-3-yl]-benzyl alcohol was prepared from 4-[3-(trifluoromethyl)-3*H*-diazirin-3-yl]benzoic acid (**1**) by reduction with borane. 4(Hydroxymethyl)benzophenone was prepared by hydrolysis of 4-(bromomethyl)benzophenone (**5**) with calcium carbonate. The two alcohols were coupled with the carboxyl group-containing component in the presence of carbodiimide and the nucleophilic catalyst (dimethylamino)pyridine. Radiolabeled probes were synthesized from [^{3}H]etomidate using a procedure similar to that used for the preparation of the unlabeled agents.

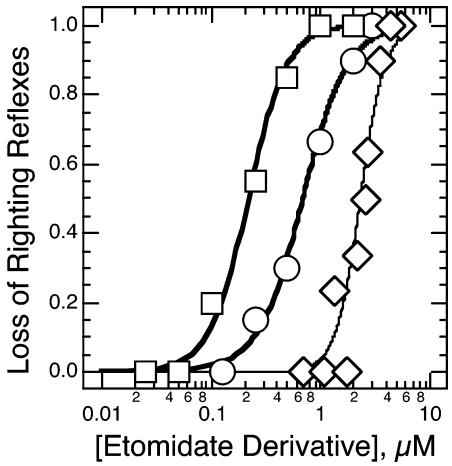

Figure 1. General anesthetic potency of BzBzl−etomidate and TDBzl−etomidate. *Xenopus* tadpoles were equilibrated with the anesthetics before checking their loss of righting reflex (LORR). For clarity, at each concentration individual experiments were pooled to give groups of 5−20 tadpoles. The total number of animals, the EC_{50} (μM), and the slopes of the dose−response curves of the drugs investigated were as follows (errors are standard deviations, SD): TDBzl−etomidate (circles), 90, 0.7 ± 0.1, and 2.2 ± 0.4; BzBzl−etomidate (squares), 100, 0.22 ± 0.03, and 2.5 ± 0.5. For comparison the EC_{50}'s of *R*-etomidate (diamonds, thin line) and *R*-azietomidate were previously determined to be 2.3 and 2.2 μM, respectively (ref 11).

Results

General Anesthetic Potency. The tadpole is a traditional animal for measuring in vivo general anesthetic potency when limited quantities of material are available. The concentration−response curves of TDBzl−etomidate and BzBzl−etomidate for loss of righting reflex (LORR) in *Xenopus* tadpoles are shown in Figure 1. Both derivatives proved to be more potent (EC_{50} values of 0.7 ± 0.1 μM and 0.22 ± 0.03 μM, respectively) than *R*-etomidate and *R*-azietomidate (EC_{50}'s of 2.3 ± 0.1 and 2.2 ± 0.1 μM, respectively).[11] All animals exposed to the anesthetic fully recovered from it when left in freshwater overnight, but at the highest concentrations toxicity was observed. Groups in which any animals died overnight were excluded from the analysis. Toxicity was apparent at and above ~2 μM for TDBzl−etomidate and 4 μM for BzBzl−etomidate. All animals exposed to 6 μM of either agent died.

The saturated aqueous solubilities in 10 mM Tris, pH 7.4, of BzBzl−etomidate and TDBzl−etomidate were 37 and 90 μM, respectively. The octanol/water partition coefficients of TDBzl−etomidate and BzBzl−etomidate were estimated to be 19 000 and 25 000, respectively, with estimated errors of 15%. Because of the high partition coefficients, the radioactivity remaining in the aqueous phase was dominated by water-soluble impurities that eluted with shorter retention times than the expected compounds. These impurities were ~0.2% of the sum of the counts in both phases, but 97% of the aqueous sample.

Potentiation of GABA-Evoked Currents. All experiments on GABA-ergic gating were carried out on *Xenopus* oocytes expressing human $\alpha_1\beta_2\gamma_{2L}$ $GABA_A$ receptor subunits using two-microelectrode voltage clamp electrophysiology. Currents stimulated with partially activating concentrations of GABA (10 μM ≈ EC_{10}) were enhanced by etomidate (diamonds, Figure 2A) at concentrations above 0.1 μM and increased monotonically up to a 10-fold enhancement at 10 μM. In comparison, both of

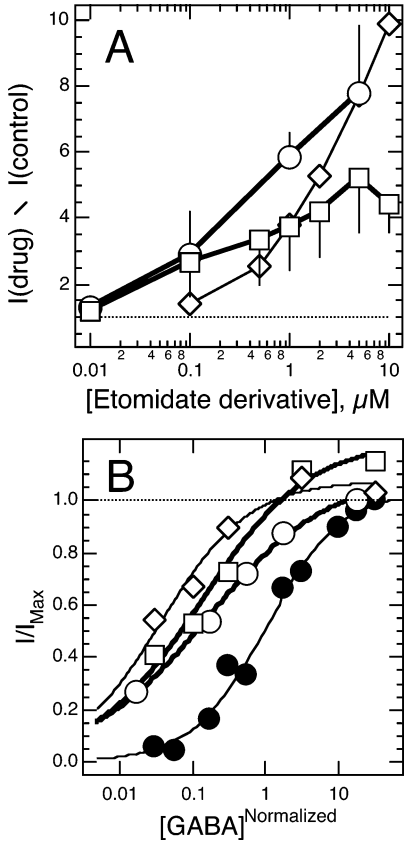

Figure 2. TDBzl−etomidate and BzBzl−etomidate enhance GABA-induced currents. *Xenopus* oocytes expressing human $\alpha_1\beta_2\gamma_{2L}$ $GABA_A$ receptor subunits were voltage clamped using two-microelectrode electrophysiology. (A) Currents elicited by 10 μM GABA ($\sim EC_{10}$) are enhanced in a concentration-dependent fashion by TDBzl−etomidate (circles), BzBzl−etomidate (squares), and etomidate (diamonds). (B) GABA concentration−response curves (filled circles) are shifted to the left by all three etomidate derivatives: 1 μM TDBzl−etomidate (open circles), 3 μM BzBzl−etomidate (squares), and 3 μM etomidate (diamonds). The GABA concentration has been normalized to the control EC_{50} of each experiment to account for systematic variation (see the Results section). The curves were fit to a logistic function. The EC_{50}, slope, and maximum current (all ± SD) were as follows: control 1.0 ± 0.2, 0.85 ± 0.09, 1.04 ± 0.04; 1 μM etomidate (not shown) 0.6 ± 0.2, 0.8 ± 0.2, 1.07 ± 0.01; 1 μM TDBzl−etomidate 0.16 ± 0.03, 0.53 ± 0.05, 1.10 ± 0.04; 3 μM BzBzl−etomidate 0.13 ± 0.05, 0.6 ± 0.1, 1.23 ± 0.08; 3 μM etomidate 0.04 ± 0.01, 0.7 ± 0.2, 1.08 ± 0.05.

the new agents were more potent, causing nearly 3-fold enhancement at 0.1 μM. However, their efficacy at high concentrations was not greater than that of etomidate. For example, at 5 μM, TDBzl−etomidate was as efficacious as etomidate, but BzBzl−etomidate had the lowest efficacy of the group. TDBzl−etomidate up to 1 μM and BzBzl−etomidate up to 10 μM did not elicit currents in the absence of GABA.

Potentiation was further characterized by determining GABA concentration−response curves at fixed anesthetic concentration (Figure 2B). Because the GABA EC_{50} varied from ∼30−60 μM between oocytes, the GABA concentration was normalized to its EC_{50} for each oocyte in order to display combined data from different experiments. Etomidate at 1 μM produced a 2-fold reduction in EC_{50} (not shown), while 1 μM TDBzl−etomidate caused a 6-fold decrease in GABA EC_{50}. On the other hand, 3 μM BzBzl−etomidate caused a smaller shift than did 3 μM etomidate (8- vs 28-fold). Only 3 μM BzBzl−etomidate caused a small but clear increase in the current elicited by maximally activating concentrations of GABA (1.23 ± 0.08-fold).

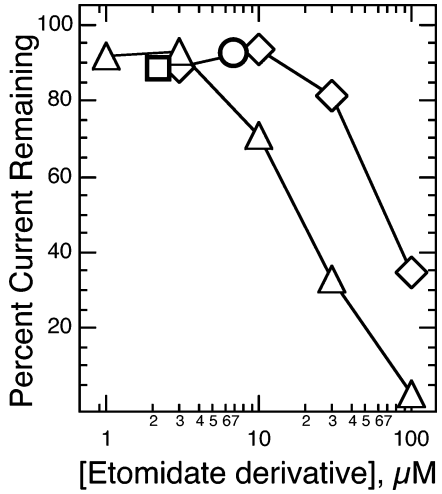

Figure 3. The 5-HT_{3A} receptor is not inhibited at clinical concentrations by any of the etomidate derivatives. Experiments were carried out in voltage clamped *Xenopus* oocytes using two-microelectrode electrophysiology. TDBzl−etomidate and BzBzl−etomidate caused minimal inhibition at the concentrations examined, but etomidate and azietomidate were more effective. The data could be fit to a logistic function to give IC_{50}'s of 70 ± 9 and 18 ± 2 μM and Hill coefficients of −1.7 ± 0.3 and −1.5 ± 0.2, respectively. Symbols: TDBzl−etomidate (circles); BzBzl−etomidate (squares); azietomidate (diamonds); 3 μM etomidate (triangles).

Inhibition of the 5-HT_{3A} Receptors. At 10 times their anesthetic EC_{50}, TDBzl−etomidate (7 μM) and BzBzl−etomidate (2.2 μM) caused little inhibition of currents induced by a maximally activating concentration of serotonin (100 μM; Figure 3). Etomidate and azietomidate did inhibit currents induced by 100 μM serotonin but only at concentrations above 10 μM. Their IC_{50}'s are 30 and 8 times their respective anesthetic EC_{50}'s. Our value for etomidate is consistent with those in the literature.[21,22] Thus, none of these agents caused significant effects on 5-HT_{3A} receptors at clinical concentrations. At the maximum concentrations shown in Figure 3, there was no evidence for an enhancing action by any of these agents at a submaximal concentration of serotonin (1 μM; ∼EC10, data not shown). This is not surprising because such an action is limited to general anesthetics smaller than these.[23]

Allosteric Regulation of $GABA_A$ Receptor Ligand Binding. To compare their allosteric action, the effects of various concentrations of etomidate and its derivatives on 1 nM [^{3}H]-flunitrazepam binding to cerebral cortex membranes were examined. As shown in Figure 4, parts A and B, all the derivatives enhanced [^{3}H]flunitrazepam binding at concentrations up to 10 μM, but only etomidate and azietomidate caused a subsequent decrease. Etomidate enhanced binding at concentrations ≥ 1 μM, whereas the derivatives did so at concentrations ≥ 0.3, 1, and 0.1 μM for azi−, TDBzl−, and BzBzl−etomidate, respectively ($P < 0.01$ compared to control (no etomidate) group, unpaired *t*-test). With the exception of etomidate, enhancement reached a clear plateau of ∼1.3−1.4-fold by 10−30 μM. For the agents exhibiting plateaus, the concentration dependence of enhancement could be fit to logistic curves, yielding half-effect concentrations of 0.80 ± 0.08, 4.5 ± 0.9, and 1.1 ± 0.3 μM for azietomidate, TDBzl−etomidate, and BzBzl−etomidate, respectively.

In the inhibition phase, 100 μM etomidate was more effective than azietomidate at reducing [^{3}H]flunitrazepam binding to a

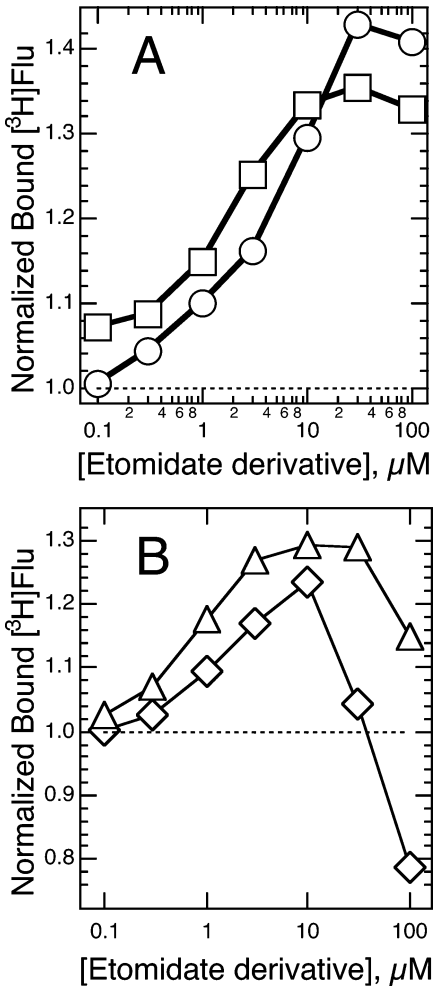

Figure 4. TDBzl−etomidate and BzBzl−etomidate allosterically enhance [^{3}H]flunitrazepam binding to GABA receptors. (A) TDBzl−etomidate (circles) and BzBzl−etomidate (squares) both enhance, whereas (B) etomidate (diamonds) and azietomidate (triangles) both exert a biphasic action on flunitrazepam binding to brain GABA receptors. Membranes from bovine cerebral cortex were incubated with 1 nM [^{3}H]flunitrazepam and various concentrations of etomidate derivatives for 1 h.

level below the control group (78.5 ± 0.4%, mean ± standard error) compared to 115 ± 2%. The other derivatives caused no significant decrease at the highest concentration examined.

Photoincorporation into the *Torpedo* nAcChoR. Photoincorporation of [^{3}H]BzBzl−etomidate (Figure 5, parts A and B) and [^{3}H]TDBzl−etomidate (Figure 5, parts C and D) into *Torpedo* nAcChoR-rich membranes was evaluated by SDS−PAGE followed by fluorography (Figure 5, parts A and C) or by liquid scintillation counting of the excised gel bands (Figure 5, parts B and D). In a typical *Torpedo* membrane preparation, nAcChoRs constitute about 10−20% of the protein, whereas other prominent polypeptides include rapsyn, a 43 kDa peripheral protein that binds to the cytoplasmic projection of the nAcChoR, polypeptides from contaminating membranes from the noninnervated surface of the electrocyte (90 kDa α-subunit of the Na^+/K^+−ATPase), and mitochondrial membrane fragments enriched in the 34 kDa voltage-dependent anion channel (VDAC).[24]

For nAcChoR-rich membranes photolabeled by [^{3}H]BzBzl−etomidate in the presence of carbamylcholine, ^{3}H incorporation was seen predominantly within the nAcChoR α-, γ-, and δ-subunits. In the presence of agonist, the photolabeling in the γ- and δ-subunits was enhanced by ∼100% and ∼80%,

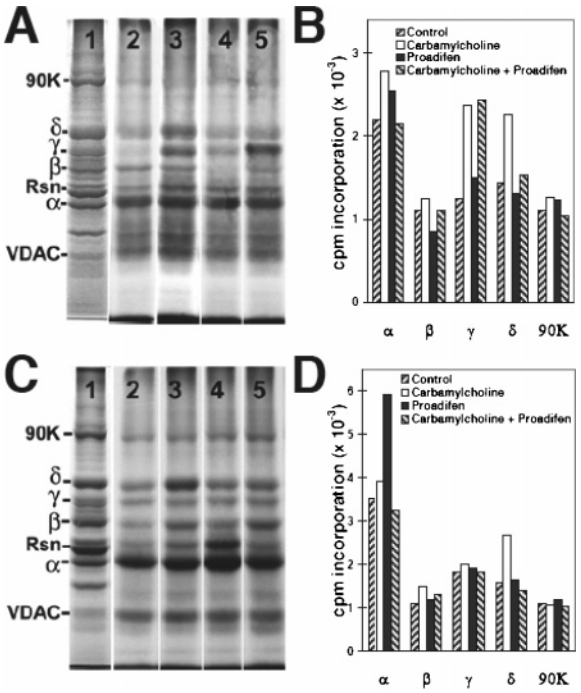

Figure 5. Photolabeling of *Torpedo* nAcChoR-rich membranes with [^{3}H]BzBzl−etomidate (panels A and B) or [^{3}H]TDBzl−etomidate (panels C and D). The photolabeled polypeptides were resolved by SDS−PAGE, and the gels processed for fluorography (4−6 weeks of exposure) (panels A and C) or ^{3}H incorporation into individual polypeptides were quantified by liquid scintillation counting of the excised protein bands (panels B and D). For panels A and C: lane 1, polypeptides as visualized by coomassie blue stain; lane 2, control, absence of carbamylcholine and proadifen; lane 3, presence of carbamylcholine; lane 4, presence of proadifen; lane 5, presence of both carbamylcholine and proadifen. Also indicated are the stained bands corresponding to the nAcChoR subunits (α, *β*, *γ*, *δ*), rapsyn (Rsn), the α-subunit of the Na^+/K^+−ATPase (90 K), and mitochondrial chloride channel (VDAC).

respectively, compared to the absence of agonist (control), while the labeling of the α-subunit was increased by ∼25%. The agonist-enhanced labeling of the α- and *δ*-subunits was reduced to control levels by the noncompetitive antagonist proadifen (100 *μ*M), which binds to a site within the nAcChoR ion channel. In contrast, the agonist-enhanced labeling of the *γ*-subunit was not inhibited by proadifen. The presence of carbamylcholine or proadifen altered photolabeling of the nAcChoR *β*-subunit by ∼10−15%, the same level of variability seen for the ^{3}H incorporation into the 90 KDa α-subunit of the Na^+/K^+−ATPase, which we take as a measure of the intrinsic variability in the analysis of ^{3}H incorporation by gel slice analysis.

Photolabeling by [^{3}H]TDBzl−etomidate revealed that carbamylcholine enhanced labeling selectively in the *δ*-subunit by 60%, while proadifen, but not carbamylcholine, increased labeling in the α-subunit by ∼70%. Both the proadifen-enhanced labeling in the *δ*-subunit and the agonist-enhanced labeling in the α-subunit were reduced to control levels in the presence of carbamylcholine and proadifen. Photolabeling within the *β*- and *γ*-subunits appeared unaffected by the presence of either drug.

In addition to photolabeling in the nAcChoR subunits, inspection of the fluorograms also reveals carbamylcholine- and proadifen-insensitive photolabeling of VDAC by both probes. In addition, [^{3}H]TDBzl−etomidate photolabeled a polypeptide whose mobility was close to that of rapsyn. However, because the pharmacological specificity of that photolabeling was the same as that of the adjacent nAcChoR α-subunit, we suspect that the most of the ^{3}H is incorporated in a photolabeled

Table 1. Pharmacology of Etomidate and Its Photoactivable Derivatives

agent	general anesthesia $^{LORR}EC_{50}$ (μM)[a]	enhancement of EC_{10} GABA currents at $^{LORR}EC_{50}$[b]	enhancement of flunitrazepam binding at $^{LORR}EC_{50}$[c]	percent inhibition of 5-HT_3R at $^{LORR}EC_{50}$[d]
etomidate	2.3	~9[5]	1.15	11
azietomidate	2.2	5.5	1.25	8
TDBzl−etomidate	0.7	5.4	1.07	<10
BzBzl−etomidate	0.22	3.0	1.08	<10

[a] $^{LORR}EC_{50}$ is the concentration at which 50% of tadpoles lost their righting reflexes (Figure 1); standard deviations are ≤15% of the mean. [b] Interpolated from data in Figure 2A; errors are ~30%. [c] Data from Figure 3 was fitted to a logistic function, except for etomidate where inhibition at high concentration prevented this and the figure is interpolated; errors are estimated as ± 0.02. [d] From data in Figure 4; errors are estimated as ± 5.

α-subunit of altered mobility, as was seen previously for nAcChoRs photolabeled with [^{3}H]*d*-tubocurarine.[25]

Discussion

General Anesthetic Properties. Both the new derivatives were typical reversible general anesthetics in tadpoles, and they were considerably more potent than either etomidate or azietomidate. Thus, a large substituent at this position on the etomidate backbone appears to be well tolerated, and the associated increase in hydrophobicity increased anesthetic potency. This is consistent with the report that in rats the nature of the ester group caused relatively minor 2−3-fold variations in potency. However, the larger structural variation examined in our work resulted in larger increases (≤10-fold) compared to those of etomidate. Although BzBzl−etomidate with an EC_{50} of 220 nM is the most potent nonsteroidal agent that we are aware of, such potency is not unprecedented. In a recent survey of 22 propofol analogues in tadpoles, the most potent was 2,6-di-*sec*-butylphenol with an EC_{50} 0f 400 nM in tadpoles.[26]

Actions on Ligand-Gated Ion Channels. The large substituents did, however, change actions at the $\alpha_1\beta_2\gamma_{2L}$ $GABA_A$ receptor. Most notably these agents, unlike etomidate and azietomidate,[11] were unable to gate the receptor in the absence of agonist. However, such gating actions occur at supraclinical concentrations, whereas the ability to enhance the response to low concentrations of agonist and to shift the GABA concentration−response curve to the left are seen at clinical concentrations. All the agents shared this action (Figure 2, parts A and B). Consistent with their higher general anesthetic potency, TDBzl−etomidate and BzBzl−etomidate both had lower threshold concentrations than etomidate for enhancing submaximal GABA currents, and at concentrations up to 1μM, both compounds caused larger reductions in GABA EC_{50} than did etomidate. When compared at their general anesthetic EC_{50}'s, both azietomidate and TDBzl−etomidate enhanced EC_{10} currents by about 5.5-fold (Table 1), whereas enhancement by BzBzl−etomidate was only 3.0-fold.

In the clinical concentration range, all four agents enhanced flunitrazepam binding, although at higher concentrations TDBzl−etomidate and BzBzl−etomidate lacked the ability to decrease its binding. However, this might simply reflect solubility limitations. Such allosteric modulation of GABA, benzodiazepine, and picrotoxin-like binding by anesthetics has been shown to parallel general anesthetics' ability both to enhance $GABA_A$ receptor function in vitro and to produce CNS depression in vivo.[27]

Overall, TDBzl−etomidate and BzBzl−etomidate resemble etomidate in their actions on $GABA_A$ receptors at clinical concentrations and thus have the potential to be useful agents for photolabeling the etomidate binding sites on this receptor. Furthermore, because they lack some of the additional pharmacological properties that etomidate and azietomidate exert on $GABA_A$ receptors at higher concentrations, they may well be more selective photolabels than azietomidate.

Etomidate is also characterized by the ability to inhibit the cation-conducting channels of the Cys-loop superfamily, the nicotinic and 5-HT_{3A} receptors, but it only does so at supraclinical levels. For the 5-HT_{3A} receptor, we found that etomidate and azietomidate had IC_{50}'s of 70 and 18 μM, 30- and 8-fold above their anesthetic concentrations, respectively. TDBzl−etomidate and BzBzl−etomidate were more selective, causing no inhibition up to 10 times their general anesthetic EC_{50}'s. Thus, all four etomidates cause no more than modest (≤10%) inhibition of 5-HT_{3A} receptors at clinical concentrations.

Photoincorporation into the nAcChoR. The $GABA_A$ receptor has such low abundance in brain that determining which amino acid residues are photolabeled presents a formidable challenge that is beyond the scope of this manuscript.[28,29] In contrast, the abundant *Torpedo* nAcChoR has been the subject of many detailed photolabeling studies, the results of which have proved useful when extrapolated to the other members of the superfamily, particularly since the determination of the nAcChoR's complete structure at a resolution of ~4 Å.[30] Thus, examining the ability of [^{3}H]TDBzl−etomidate and [^{3}H]BzBzl−etomidate to photolabel the nAcChoR is an important step in assessing their utility as a photoaffinity reagents.

TDBzl−etomidate and BzBzl−etomidate photolabeled all the nAcChoR subunits as well as other polypeptides in the membrane suspension. However, the important point is that only in certain nAcChoR subunits, and never in the other polypeptides, was the level of photoincorporation modulated pharmacologically by the agonist, carbamylcholine, or the channel blocker, proadifen. In the case of TDBzl−etomidate, photoincorporation into the α-subunit was enhanced by the presence of proadifen, and this enhanced photolabeling was inhibited by carbamylcholine. By contrast, in the δ-subunit it was carbamylcholine that caused enhancement of photolabeling that was inhibited by proadifen. In the case of BzBzl−etomidate, carbamylcholine enhanced photoincorporation into the γ- and δ-subunits by ~100%, with the agonist-enhanced labeling in the δ-subunit being inhibited by proadifen, whereas that in the γ-subunit was insensitive. These complex pharmacological specificities of subunit photolabeling have parallels with that seen for [^{3}H]azietomidate, for which the agonist-enhanced labeling seen in the α-subunit resulted from photolabeling in the ion channel domain, whereas the proadifen-enhanced labeling seen in the δ-subunit resulted from photoincorporation in the agonist binding site.[13] Much more detailed work, beyond the scope of this study, will be required to establish if this is the case for TDBzl−etomidate and BzBzl−etomidate.

Overall, for photolabeling carried out at 1 μM [^{3}H]TDBzl−etomidate and [^{3}H]BzBzl−etomidate, the pharmacologically sensitive photolabeling of the nAcChoR subunits was at a level of ~0.1% of nAcChoRs, an efficiency of photoincorporation similar to that seen for [^{3}H]azietomidate at the same concentra-

tion.[13] However, further studies at higher drug concentrations are required to determine photolabeling efficiency when binding sites are fully occupied, and direct identification of the labeled amino acids will be necessary to determine the actual side chain preferences for these novel etomidate photoprobes. When extrapolating to future photolabeling studies of $GABA_A$ receptors, the higher affinity of the new agents will lead to greater occupancy at a given concentration, likely resulting in higher fractions of specific photoincorporation.

Conclusion. We have synthesized and characterized the pharmacology of two potent new general anesthetics that are photoactivable etomidate derivatives able to insert into the nAcChoR in an allosterically regulated manner. These agents also enhance agonist-stimulated currents with high selectivity and potency in their likely physiological target, the $GABA_A$ receptor, a member of the same superfamily as the nAcChoR. Thus, they have the necessary pharmacological and photochemical properties to be useful in identifying the site of etomidate-induced anesthesia.

Experimental Section

Materials and Methods. Anhydrous dichloromethane, diisopropylcarbodiimide, *p*-(dimethyamino)pyridine, and Merck silica gel 60 A, 230−400 mesh were obtained from Aldrich (Milwaukee, WI). 4-[3-(Trifluoromethyl])-3*H*-diazirin-3-yl]benzoic acid was obtained from Bachem (King of Prussia, PA). *R*(+)-etomidate was a kind gift from Organon Laboratories (Newhouse, Lancashire, Scotland). *R*(+)etomidate used in $GABA_A$ receptor electrophysiology studies was purchased from Bedford Laboratories (Bedford, OH) as a 2.0 mg/mL solution in 35% propylene glycol/water (v/v). All other chemicals were from Sigma (St. Louis, MO). cDNAs for the α_1, β_2, and γ_{2L} subunits of human $GABA_A$ receptors in pCDM8 vectors were gifts from Dr. Paul J. Whiting (Merck Sharp & Dohme Research Labs, Essex, U.K.).

^{1}H NMR spectra were recorded on a JEOL Eclipse 400 MHz spectrometer in $CDCl_3$ with tetramethylsilane as reference by Acorn NMR Spectroscopy Service, Livermore, CA. UV spectra were recorded on a Hewlett-Packard spectrophotometer. HPLC analysis was performed on a Varian Prostar instrument with a C-18 reversed-phase column (Varian, Walnut Creek, CA).

Preparation of 4-[3-(Trifluoromethyl)-3*H*-diazirin-3-yl]benzyl Alcohol (2). A 1 M solution of diborane in THF (2.4 mL) was added dropwise over a period of 40 min to a solution of 4-[3-(trifluoromethyl)-3*H*-diazirin-3-yl]benzoic acid **1** (92 mg) in anhydrous THF (1 mL) under argon at −5 °C. Stirring was continued for 5 h at −5 °C. The solution was slowly quenched by adding 10% acetic acid in methanol (1 mL). The mixture was rotary evaporated, and the residue was dissolved in dichloromethane and applied to a column of silica gel, equilibrated with dichloromethane. Elution was performed successively with dichloromethane and a mixture of 2.5% ether in dichloromethane, yielding the alcohol **2** (68 mg, 78% yield). NMR ($CDCl_3$) δ 4.63 (s, 2H), 7.23 (d, 2H, aromatic), 7.46 (d, 2H, aromatic). UV spectrum (methanol) λ_{max} 360 nm, ϵ = 309 M^{-1} cm^{-1}. Elemental analysis. Calcd for $C_9H_7F_3N_2O$: C, 50.00%; H, 3.27%; N, 12.96%. Found: C, 49.29%; H, 3.28%; N, 12.44%.

Preparation of *R*-1-(1-Phenylethyl)-1*H*-imidazole-5-carboxylic Acid (3). The carboxylic acid derivative **3** was prepared from *R*-2-ethyl-1-(1-phenylethyl)-1*H*-imidazole-5-carboxylate (etomidate) by alkaline hydrolysis as described previously.[11]

Preparation of *R*-4-[3-(Trifluoromethyl)-3*H*-diazirin-3-yl]-benzyl-1-(1-phenylethyl)-1*H*-imidazole-5-carboxylate (4). A mixture of *R*-1-(1-phenylethyl)-1*H*-imidazole-5-carboxylic acid **3** (0.2 mmol), 4-[3-(trifluoromethyl)-3*H*-diazirin-3-yl]benzyl alcohol **2** (48 mg, 0.2 mmol), and (dimethylamino)pyridine (24 mg, 0.2 mmol) in anhydrous dichloromethane (0.5 mL) was stirred with diisopropylcarbodiimide (47 μL, 0.3 mmol) overnight at room temperature. The reaction mixture was purified by silica gel chromatography with 5% diethyl ether in dichloromethane, yielding an oily residue of **4** (37 mg, 45% yield). The product was converted to crystalline solid hydrochloride by acidification with HCl in ether. NMR ($CDCl_3$) δ 1.95 (d, 3H), 5.36 (s, 2H), 6.36 (q, 1H), 7.28 (m, 4H, aromatic), 7.35 (m, 3H, aromatic), 7.46 (m, 2H, aromatic), 7.65 (m, 1H), 7.75 (m, 5H), 8.32 (s, 1H), 9.29 (s, 1H). UV spectrum (methanol) λ_{max} 355 nm, ϵ = 310 M^{-1} cm^{-1}. Elemental analysis. Calcd for $C_{21}H_{18}ClF_3N_4O_2 \cdot H_2O$: C, 53.79%; H, 4.30%; N, 11.95%. Found: C, 53.08%; H, 4.26%; N, 11.53%.

Preparation of 4(Hydroxymethyl)benzophenone (6). 4-(Bromomethyl)benzophenone **5** (2.75 g, 10 mmol) in dioxane (25 mL) was mixed with a suspension of calcium carbonate powder (5 g, 50 mmol) in water (25 mL) and refluxed for 20 h. The solvent was removed by rotary evaporation, and the residue was suspended in dichloromethane (30 mL) and carefully treated with 1 M HCl until the residue dissolved. The organic layer was separated, washed with water, and dried over magnesium sulfate. The solvent was removed by rotary evaporation, and the residue was purified on a column of silica with 10% ether in dichloromethane, yielding the hydroxy compound **6** (0.65 g, 31% yield). NMR ($CDCl_3$) δ 4.72 (s, 2H), 7.64 (m, 2H), 6.36 (q, 1H), 7.18 (m, 2H), 7.30 (m, 3H), 7.53 (m, 4H), 7.65 (m, 1H), 7.75 (m, 9H). UV spectrum (methanol) λ_{max} 330 nm, ϵ = 206 M^{-1} cm^{-1}. Elemental analysis. Calcd for $C_{14}H_{12}O_2$: C, 79.23%; H, 5.70%. Found: C, 79.41%; H, 5.81%.

Preparation of *R*-4-Benzoylbenzyl-1-(1-phenylethyl)-1*H*-imidazole-5-carboxylate (7). The benzobenzyl derivative **7** was synthesized from hydroxybenzophenone **2** (48 mg, 0.22 mmol) and *R*-1-(1-phenylethyl)-1*H*-imidazole-5-carboxylic acid (0.2 mmol) by a procedure similar to that described for the preparation of TDBzl−etomidate, **4**. The reaction mixture was purified by silica gel chromatography and by HPLC, yielding 23 mg (25% yield) of BzBzl−etomidate **7**. NMR ($CDCl_3$) δ 1.90 (d, 3H), 5.36 (s, 2H), 6.36 (q, 1H), 7.18 (m, 2H), 7.30 (m, 3H), 7.53 (m, 4H), 7.65 (m, 1H), 7.75 (m, 5H), 8.18 (s, 1H). UV spectrum (methanol) λ_{max} 331 nm, ϵ = 215 M^{-1} cm^{-1}. Elemental analysis. Calcd for $C_{26}H_{23}ClN_2O_3 \cdot H_2O$: C, 67.17%; H, 5.42%; N, 6.02%. Found: C, 67.64%; H, 5.47%; N, 6.09%.

Preparation of *R*-[^{3}H]-4-[3-(Trifluoromethyl])-3*H*-diazirin-3-yl]benzyl-1-(1-phenylethyl)-1*H*-imidazole-5-carboxylate (4). *R*-Etomidate was tritiated to a specific activity of 20 Ci/mmol and converted by alkaline hydrolysis to *R*-[^{3}H]1-(1-phenylethyl)-1*H*-imidazole-5-carboxylic acid as described earlier.[11] A mixture of *R*-[^{3}H]1-(1-phenylethyl)-1*H*-imidazole-5-carboxylic acid (8.8 mCi), 4-[3-(trifluoromethyl)-3*H*-diazirin-3-yl]benzyl alcohol **2** (23 μmol), (dimethylamino)pyridine (10 μmol), and (dimethylamino)pyridine hydrochloride (10 μmol) in anhydrous dichloromethane (0.6 mL) was stirred with diisopropylcarbodiimide (20 μL of 1 M solution) for 24 h at room temperature. The reaction mixture was purified by chromatography on a silica gel column equilibrated with dichloromethane and eluted successively with dichloromethane and with dichloromethane containing 5% ether.

Preparation of *R*-[^{3}H]4-Benzoylbenzyl-1-(1-phenylethyl)-1*H*-imidazole-5-carboxylate (7). Tritiated benzoylbenzyl derivative of etomidate was synthesized by a procedure similar to that described for the synthesis of labeled trifluoromethyldiazirinyl-etomidate, **4**.

General Anesthetic Potency. With institutional approval, general anesthetic potency was assessed in prelimb bud *Xenopus* tadpoles, 1.5−2 cm in length (Xenopus 1, Inc., Dexter, MI). Groups of five tadpoles were placed in covered 100 mL glass beakers or square slide-staining dishes in oxygenated aqueous solutions buffered with 2.5 mM Tris HCl at pH 7.4 under low levels of ambient light. Agents were added from stock solutions in ethanol. The final concentration of ethanol did not exceed 5 mM, a concentration that does not contribute to anesthesia.[31] Tadpoles were tipped manually with a flame polished pipet, and failure to right after 5 s was defined as loss of righting reflexes (LORR). The response stabilized within 30−40 min, and measurements were made at 50−60 min. All animals were placed in freshwater and observed the next day for toxicity. The quantal concentration response curves were analyzed by the method of Waud[32] using an Excel macro kindly provided by N. L. Harrison, A. Jenkins, and S. P. Singh (Weill Medical College of Cornell University).

Solubility Properties. The solubility of BzBzl−etomidate and TDBzl−etomidate in 0.01 M Tris−HCl buffer, pH 7.4, was determined by stirring excess photoetomidates in the buffer for 24 h, centrifuging at 10 000*g*, and determining the concentration at 251 nm for BzBzl−etomidate and 249 nm for TDBzl−etomidate. To determine octanol/water partition coefficients, the tritiated probes were stirred in a two-phase mixture of octanol and water, aliquots were removed from the separated phases, applied to an HPLC Clipeus C-18 reversed-phase column (Higgins Analytical, Inc., Mountain View, CA), and 1 mL fractions were collected for scintillation counting. The concentration of the probe in the two phases was calculated from the radioactivity collected in samples eluting at the calibrated retention time for the unlabeled probe.

Electrophysiology of $GABA_A$ and 5-HT_{3A} Receptors. Recombinant wild-type $GABA_A$ receptors (consisting of human $\alpha_1\beta_2\gamma_{2L}$ subunits) and human 5-HT_{3A} receptors were expressed in *Xenopus laevis* oocytes as previously described.[5] Capped mRNAs were transcribed in vitro from linearized cDNA templates and stored at −80 °C prior to injection. Defolliculated stage V and VI oocytes were injected with a 50−75 nL mixture of receptor subunit mRNAs, incubated at 17 °C, and used for electrophysiological experiments for up to 7 days.

Electrophysiological experiments were performed at 22−24 °C using the whole-cell two-electrode voltage clamp technique.[33,34] Oocytes were held at a membrane potential of −50 mV and were continuously superfused with ND-96 buffer (containing in mM: 96 NaCl, 2 KCl, 10 HEPES, 1 $CaCl_2$, 0.8 $MgCl_2$, pH adjusted to 7.5 with NaOH) using a gravity-driven syringe superfusion system. Current responses were elicited by agonist/drug solution exposures between 5 and 50 s, digitized at 50−200 Hz, and recorded on a personal computer.

Agonist (GABA or 5-HT; both from Sigma Chemical Co, St. Louis, MO) solutions were prepared in ND-96. Etomidate solutions up to 100 μM were prepared by diluting commercial stock (8.2 mM in 35% poly(ethylene glycol)) in 35% propylene glycol into ND-96. The maximum concentration of propylene glycol was 60 mM, which had no effect on agonist-activated currents with either $GABA_A$ or 5-HT_{3A} receptors. Azi−etomidate, TDBzl−etomidate, and BzBzl−etomidate solutions were prepared by diluting stock solutions in DMSO (for $GABA_A$ receptor studies) or methanol (for $5HT_{3A}$ receptor studies) with ND-96 buffer. Stock solvents at the highest concentrations used (<1%) were shown to have no effect on the respective agonist-evoked peak responses.

Allosteric Regulation of $GABA_A$ Receptor Ligand Binding. Fresh whole bovine brain was placed on ice, and the cortex was rapidly removed, immersed in 0.32 M sucrose, and frozen at −80 °C. The frozen cerebral cortex was thawed and homogenized in 0.32 M sucrose, 10 mM phosphate buffer (pH 7.4). The homogenate was centrifuged (650*g*, 10 min, 4 °C), and the supernatant was then centrifuged at 150 000*g* for 48 min. The pellet was resuspended in distilled water. The suspension was recentrifuged at 150 000*g* for 48 min, and the pellet was resuspended in 10 mM phosphate buffer (pH 7.4) and stored frozen at −80 °C. Before use, the frozen suspension was thawed, and the membranes were diluted ×10 into assay buffer (10 mM phosphate buffer (pH 7.4), 200 mM KCl, and 1 mM EDTA). Diluted membranes (400 μL) were incubated in a final volume of 0.5 mL for 1 h at 4 °C with [^{3}H]flunitrazepam (1 nM, 85.2 Ci/mmol, Perkin-Elmer Life Sciences). Nonspecific binding was determined by carrying out incubations in the presence of 7.5 μM flurezapam, and enhancement of etomidate or its derivatives was done at various concentrations (0.1, 0.3, 1, 3, 10, 30, and 100 μm) in parallel tubes. Triplicates of incubations were filtered on GF/B glass fiber filters under suction. The filters were washed with 3 mL of assay buffer twice and transferred to scintillation vials and subjected to scintillation counting after addition of 2.5 mL of scintillation fluid (Ecolume, ICN).

Photolabeling the *Torpedo* nAcChoR. nAcChoR-rich membranes, prepared from *T. californica* electric organ, were suspended at a protein concentration of 2 mg/mL in *Torpedo* physiological saline (TPS, in mM: 250 NaCl, 5 KCl, 3 $CaCl_2$, 2 $MgCl_2$, 5 NaH_2PO_4, pH 7.0) supplemented with 1 mM oxidized glutathione (pH 7) to serve as an aqueous scavenger. Membrane suspensions, shielded from light, were incubated at 4 °C for 90 min with 0.75 μM [^{3}H]BzBzl−etomidate or [^{3}H]TDBzl−etomidate in the absence or presence of the agonist carbamylcholine (1 mM), or the desensitizing noncompetitive antagonist proadifen (100 μM), or both. Aliquots of each sample (230 μg of protein; 120 pmol of nAcChoRs; in 130 μL of TPS) were irradiated on ice in a 96-well polystyrene microtiter plate (Costar no. 9017) at 365 nm at a distance of 6 cm in a horizontal photochemical chamber reactor (Rayonet RPR-200, Southern New England Ultraviolet Company, Branford, CT). On the basis of previous experience with photoincorporation of benzophenone[35] and trifluoromethylaryl diazirine[36] photoprobes into *Torpedo* nAcChoR-rich membranes, irradiation was carried out for 60 and 30 min for [^{3}H]BzBzl−etomidate and [^{3}H]TDBzl−etomidate, respectively. The photolabeled membrane suspensions were pelleted and then solubilized in electrophoresis sample-loading buffer and subjected to SDS−PAGE on 1.5 mm thick 8% polyacrylamide gels with 0.33% bisacrylamide. The polypeptides were visualized by staining with coomassie blue R-250 (0.25% w/v in 45% methanol and 10% acetic acid) and destaining in 25% methanol, 10% acetic acid. For fluorography, the gels were impregnated with fluor (Amplify, Amersham Biosciences GE Healthcare) for 30 min, dried, and exposed to film (Kodak X-Omat Blue XB-1) for 4−6 weeks. Incorporation of ^{3}H into individual polypeptides was determined by liquid scintillation counting of the protein bands excised from the stained gels.

Acknowledgment. This research was supported by a Grant from the National Institute for General Medical Sciences (GM 58448) and by the Department of Anesthesia and Critical Care, Massachusetts General Hospital. K.S. was supported by T32 GM07592. We thank Dr. David K. Gemmell, Organon Laboratories, U.K., for a kind gift of *R*(+)-etomidate.

Supporting Information Available: Results from elemental analysis. This material is available free of charge via the Internet at http://pubs.acs.org.

References

(1) Godefroi, E. F.; Janssen, P. A. J.; Van Der Eycken, C. A. M.; Van Heertum, A. H. M. T.; Niemegeers, C. J. E. DL-1-(1-Arylalkyl)-imidazole-5-carboxylate Esters. A Novel Type of Hypnotic Agents. *J. Med. Chem.* **1965**, *8*, 220−223.

(2) Tomlin, S. L.; Jenkins, A.; Lieb, W. R.; Franks, N. P. Stereoselective effects of etomidate optical isomers on gamma-aminobutyric acid type A receptors and animals. *Anesthesiology* **1998**, *88*, 708−717.

(3) Pistis, M.; Belelli, D.; Peters, J. A.; Lambert, J. J. The interaction of general anaesthetics with recombinant $GABA_A$ and glycine receptors expressed in *Xenopus laevis oocytes*: a comparative study. *Br. J. Pharmacol.* **1997**, *122*, 1707−1719.

(4) Lambert, J. J.; Belelli, D.; Shepard, S.; Muntoni, A.-L.; Pistis, M.; Peters, J. A. The GABA Receptor: An Important Locus for Intravenous Anaesthetic Action. *Gases in Medicine: Anæsthesia*; Royal Society of Chemistry: Cambridge, 1998; pp 121−137.

(5) Rüsch, D.; Zhong, H.; Forman, S. A. Gating allosterism at a single class of etomidate sites on alpha1beta2gamma2L GABA A receptors accounts for both direct activation and agonist modulation. *J. Biol. Chem.* **2004**, *279*, 20982−20992.

(6) Hill-Venning, C.; Belelli, D.; Peters, J. A.; Lambert, J. J. Subunit-dependent interaction of the general anaesthetic etomidate with the gamma-aminobutyric acid type A receptor. *Br. J. Pharmacol.* **1997**, *120*, 749−756.

(7) Belelli, D.; Lambert, J. J.; Peters, J. A.; Wafford, K.; Whiting, P. J. The interaction of the general anesthetic etomidate with the gamma-aminobutyric acid type A receptor is influenced by a single amino acid. *Proc. Natl. Acad. Sci. U.S.A.* **1997**, *94*, 11031−11036.

(8) Reynolds, D. S.; Rosahl, T. W.; Cirone, J.; O'Meara, G. F.; Haythornthwaite, A.; Newman, R. J.; Myers, J.; Sur, C.; Howell, O.; Rutter, A. R.; Atack, J.; Macaulay, A. J.; Hadingham, K. L.; Hutson, P. H.; Belelli, D.; Lambert, J. J.; Dawson, G. R.; McKernan, R.; Whiting, P. J.; Wafford, K. A. Sedation and anesthesia mediated by distinct GABA(A) receptor isoforms. *J. Neurosci.* **2003**, *23*, 8608−8617.

(9) Jurd, R.; Arras, M.; Lambert, S.; Drexler, B.; Siegwart, R.; Crestani, F.; Zaugg, M.; Vogt, K. E.; Ledermann, B.; Antkowiak, B.; Rudolph, U. General anesthetic actions in vivo strongly attenuated by a point mutation in the GABA(A) receptor beta3 subunit. *FASEB J.* **2003**, *17*, 250−252.
(10) Peters, J. A.; Lambert, J. J. Anaesthetics in a bind? *Trends Pharmacol. Sci.* **1997**, *18*, 454−455.
(11) Husain, S. S.; Ziebell, M. R.; Ruesch, D.; Hong, F.; Arevalo, E.; Kosterlitz, J. A.; Olsen, R. W.; Forman, S. A.; Cohen, J. B.; Miller, K. W. 2-(3-Methyl-3*H*-diaziren-3-yl)ethyl 1-(1-phenylethyl)-1*H*-imidazole-5-carboxylate: a derivative of the stereoselective general anesthetic etomidate for photolabeling ligand-gated ion channels. *J. Med. Chem.* **2003**, *46*, 1257−1265.
(12) Liao, M.; Sonner, J. M.; Husain, S. S.; Miller, K. W.; Jurd, R.; Rudolph, U.; Eger, E. I., II. *R*(+)-etomidate and the photoactivable *R*(+)-azietomidate have comparable anesthetic activity in wild-type mice and comparably decreased activity in mice with a N265M point mutation in the gamma-aminobutyric acid receptor beta3 subunit. *Anesth. Analg.* **2005**, *101*, 131−135.
(13) Ziebell, M. R.; Nirthanan, S.; Husain, S. S.; Miller, K. W.; Cohen, J. B. Identification of binding sites in the nicotinic acetylcholine receptor for [^{3}H]azietomidate, a photoactivatable general anesthetic. *J. Biol. Chem.* **2004**, *279*, 17640−17649.
(14) Pratt, M. B.; Husain, S. S.; Miller, K. W.; Cohen, J. B. Identification of sites of incorporation in the nicotinic acetylcholine receptor of a photoactivatible general anesthetic. *J. Biol. Chem.* **2000**, *275*, 29441−29451.
(15) Addona, G. H.; Husain, S. S.; Stehle, T.; Miller, K. W. Geometric isomers of a photoactivable general anesthetic delineate a binding site on adenylate kinase. *J. Biol. Chem.* **2002**, *277*, 25685−25691.
(16) Das, J.; Addona, G. H.; Sandberg, W. S.; Husain, S. S.; Stehle, T.; Miller, K. W. Identification of a general anesthetic binding site in the diacylglycerol-binding domain of protein kinase Cdelta. *J. Biol. Chem.* **2004**, *279*, 37964−37972.
(17) Brunner, J. New photolabeling and cross-linking methods. *Annu. Rev. Biochem.* **1993**, *62*, 483−514.
(18) Dorman, G.; Prestwich, G. D. Benzophenone photophores in biochemistry. *Biochemistry* **1994**, *33*, 5661−5673.
(19) Kotzyba-Hibert, F.; Kapfer, I.; Goeldner, M. Recent trends in photoaffinity labeling. *Angew. Chem., Int. Ed.* **1995**, *34*, 1296−1312.
(20) Li, G.; Sawyer, G. W.; Husain, S. S.; Olsen, R. W. $GABA_A$ receptor subunits were photoaffinity labeled with [^{3}H]azietomidate. Presented at the Society for Neuroscience, 34th Annual Meeting, San Diego, CA, 2004; Poster Presentation 51.58.
(21) Appadu, B. L.; Lambert, D. G. Interaction of i.v. anaesthetic agents with 5-HT_3 receptors. *Br. J. Anaesth.* **1996**, *76*, 271−273.
(22) Barann, M.; Gothert, M.; Fink, K.; Bonisch, H. Inhibition by anaesthetics of ^{14}C-guanidinium flux through the voltage-gated sodium channel and the cation channel of the 5-HT_3 receptor of N1E-115 neuroblastoma cells. *Naunyn−Schmiedebergs Arch. Pharmacol.* **1993**, *347*, 125−132.
(23) Stevens, R. J.; Rüsch, D.; Davies, P. A.; Raines, D. E. Molecular properties important for inhaled anesthetic action on human 5-HT_{3A} receptors. *Anesth. Analg.* **2005**, *100*, 1696−1703.
(24) Blanton, M. P.; Lala, A. K.; Cohen, J. B. Identification and characterization of membrane-associated polypeptides in *Torpedo* nicotinic acetylcholine receptor-rich membranes by hydrophobic photolabeling. *Biochim. Biophys. Acta* **2001**, *1512*, 215−224.
(25) Pedersen, S. E.; Cohen, J. B. D-Tubocurarine binding sites are located at alpha-gamma and alpha-delta subunit interfaces of the nicotinic acetylcholine receptor. *Proc. Natl. Acad. Sci. U.S.A.* **1990**, *87*, 2785−2789.
(26) Krasowski, M. D.; Jenkins, A.; Flood, P.; Kung, A. Y.; Hopfinger, A. J.; Harrison, N. L. General anesthetic potencies of a series of propofol analogues correlate with potency for potentiation of gamma-aminobutyric acid (GABA) current at the GABA(A) receptor but not with lipid solubility. *J. Pharmacol. Exp. Ther.* **2001**, *297*, 338−351.
(27) Olsen, R. W.; Fischer, J. B.; Dunwiddie, T. V. Barbiturate Enhancement of γ-Aminobutyric Acid Receptor Binding and Function as a Mechanism of Anesthesia. *Molecular and Cellular Mechanisms of Anesthetics*; Plenum: New York, 1986; pp 165−178.
(28) Smith, G. B.; Olsen, R. W. Deduction of amino acid residues in the GABA(A) receptor alpha subunits photoaffinity labeled with the benzodiazepine flunitrazepam. *Neuropharmacolology* **2000**, *39*, 55−64.
(29) Sawyer, G. W.; Chiara, D. C.; Olsen, R. W.; Cohen, J. B. Identification of the bovine gamma-aminobutyric acid type A receptor alpha subunit residues photolabeled by the imidazobenzodiazepine [3H]Ro15−4513. *J. Biol. Chem.* **2002**, *277*, 50036−50045.
(30) Unwin, N. Refined structure of the nicotinic acetylcholine receptor at 4 Å resolution. *J. Mol. Biol.* **2005**, *346*, 967−989.
(31) Alifimoff, J. K.; Firestone, L. L.; Miller, K. W. Anaesthetic potencies of primary alkanols: implications for the molecular dimensions of the anaesthetic site. *Br. J. Pharmacol.* **1989**, *96*, 9−16.
(32) Waud, D. R. On biological assays involving quantal responses. *J. Pharmacol. Exp. Ther.* **1972**, *183*, 577−607.
(33) Scheller, M.; Forman, S. A. The gamma subunit determines whether anesthetic-induced leftward shift is altered by a mutation at alpha1S270 in alpha1beta2gamma2L GABA(A) receptors. *Anesthesiology* **2001**, *95*, 123−131.
(34) Solt, K.; Stevens, R. J.; Davies, P. A.; Raines, D. E. General anesthetic-induced channel gating enhancement of 5-hydroxytryptamine type 3 receptors depends on receptor subunit composition. *J. Pharmacol. Exp. Ther.* **2005**, *315*, 771−776.
(35) Wang, D.; Chiara, D. C.; Xie, Y.; Cohen, J. B. Probing the structure of the nicotinic acetylcholine receptor with 4-benzoylbenzoylcholine, a novel photoaffinity competitive antagonist. *J. Biol. Chem.* **2000**, *275*, 28666−28674.
(36) Chiara, D. C.; Trinidad, J. C.; Wang, D.; Ziebell, M. R.; Sullivan, D.; Cohen, J. B. Identification of amino acids in the nicotinic acetylcholine receptor agonist binding site and ion channel photolabeled by 4-[(3-trifluoromethyl)-3*H*-diazirin-3-yl]benzoylcholine, a novel photoaffinity antagonist. *Biochemistry* **2003**, *42*, 271−283.
(37) Abbreviations: AcCho, acetylcholine; azietomidate, *R*-2-(3-methyl-3*H*-diaziren-3-yl)ethyl 1-(1-phenylethyl)-1*H*-imidazole-5-carboxylate; TDBzl−etomidate, *R*-4-[3-(trifluoromethyl])-3*H*-diazirin-3-yl]benzyl 1-(1-phenylethyl)-1*H*-imidazole-5-carboxylate; BzBzl−etomidate, *R*-4-benzoylbenzyl-1-(1-phenylethyl)-1*H*-imidazole-5-carboxylate; etomidate, 2-ethyl 1-(phenylethyl)-1*H*-imidazole-5-carboxylate; LORR, loss of righting reflexes; nAcChoR, nicotinic acetylcholine receptor; octanol, octan-1-ol; SD, standard deviation; TPS, *Torpedo* physiological saline.

JM051207B